

## Supplemental Information

### Major differences between the self-assembly and seeding behavior of heparin-induced- and in-vitro-phosphorylated tau and their modulation by potential inhibitors

Clément Despres,<sup>1,‡</sup> Jing Di,<sup>2,‡</sup> François-Xavier Cantrelle,<sup>1</sup> Zizheng Li,<sup>2</sup> Isabelle Huvent,<sup>1</sup> Béatrice Chambraud,<sup>3</sup> Jing Zhao,<sup>4</sup> Jianle Chen,<sup>4,5</sup> Shiguo Chen,<sup>5</sup> Guy Lippens,<sup>1†</sup> Fuming Zhang,<sup>6</sup> Robert Linhardt,<sup>5,6,7</sup> Chunyu Wang,<sup>6,7</sup> Frank-Gerrit Klärner,<sup>8</sup> Thomas Schrader,<sup>8</sup> Isabelle Landrieu,<sup>1</sup> Gal Bitan,<sup>2,9,10\*</sup> Caroline Smet-Nocca<sup>1\*</sup>

<sup>1</sup> Lille University CNRS UMR 8576, UGSF, F-59000 Lille, France

<sup>2</sup> Department of Neurology, David Geffen School of Medicine, University of California, Los Angeles, CA 90095, United States

<sup>3</sup> UMR 1195 Inserm, University Paris XI, Le Kremlin Bicêtre, France

<sup>4</sup> Center for Biotechnology and Interdisciplinary Studies, Rensselaer Polytechnic Institute, Troy, New York

<sup>5</sup> Department of Food Science and Nutrition, Zhejiang University, Hangzhou, Zhejiang 310029, China

<sup>6</sup> Department of Chemical and Biological Engineering, Rensselaer Polytechnic Institute, Troy, New York

<sup>7</sup> Department of Biological Sciences, Rensselaer Polytechnic Institute, Troy, New York

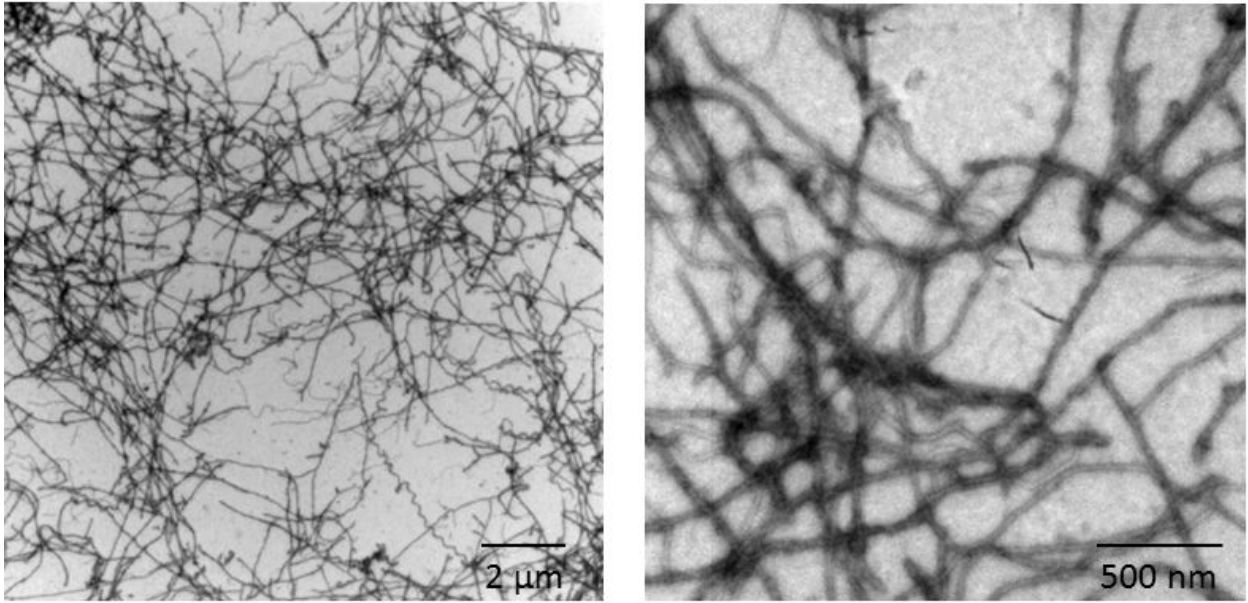
<sup>8</sup> Institute of Organic Chemistry, University of Duisburg-Essen, 45141 Essen, Germany

<sup>9</sup> Brain Research Institute, University of California, Los Angeles, CA 90095, United States

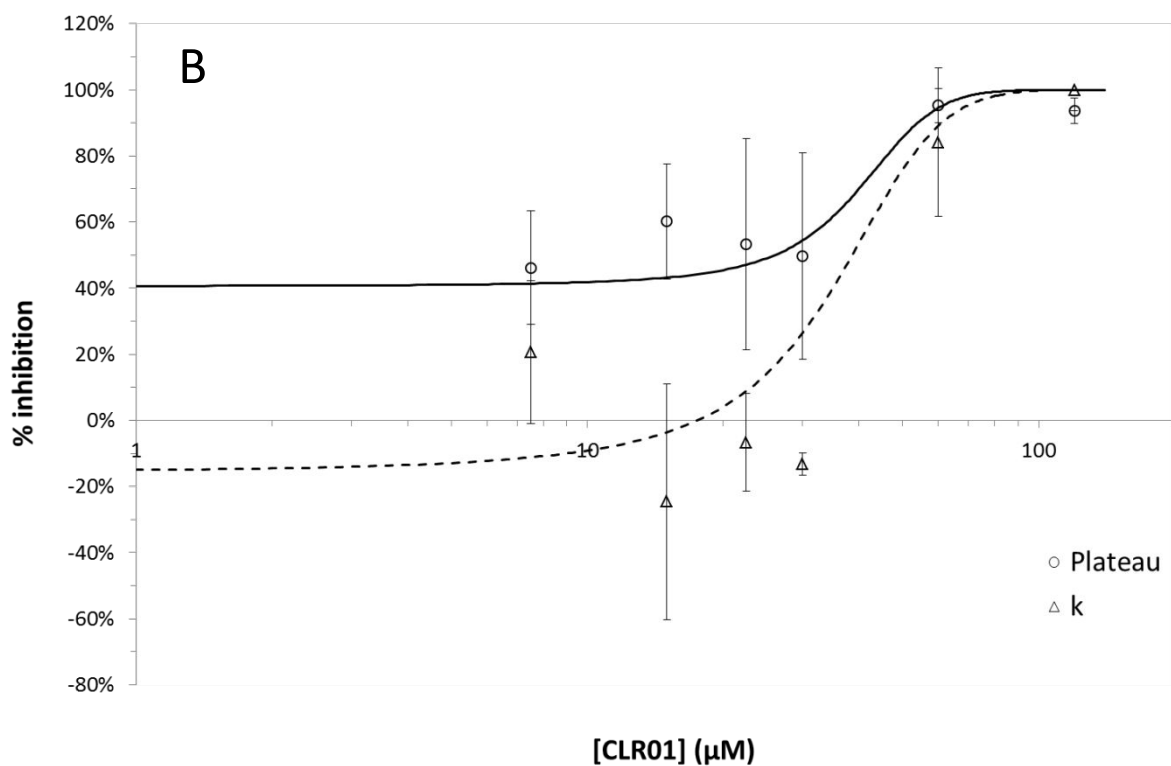
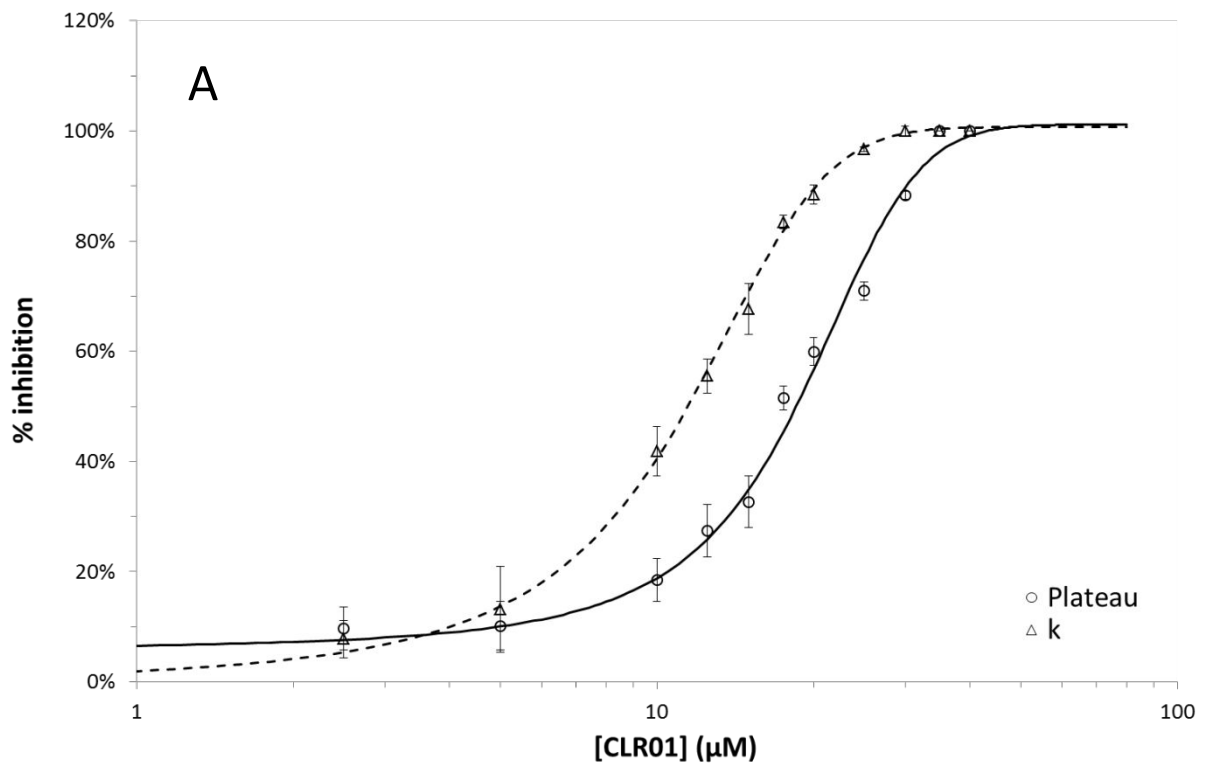
<sup>10</sup> Molecular Biology Institute, University of California, Los Angeles, CA 90095, United States

‡The authors contributed equally

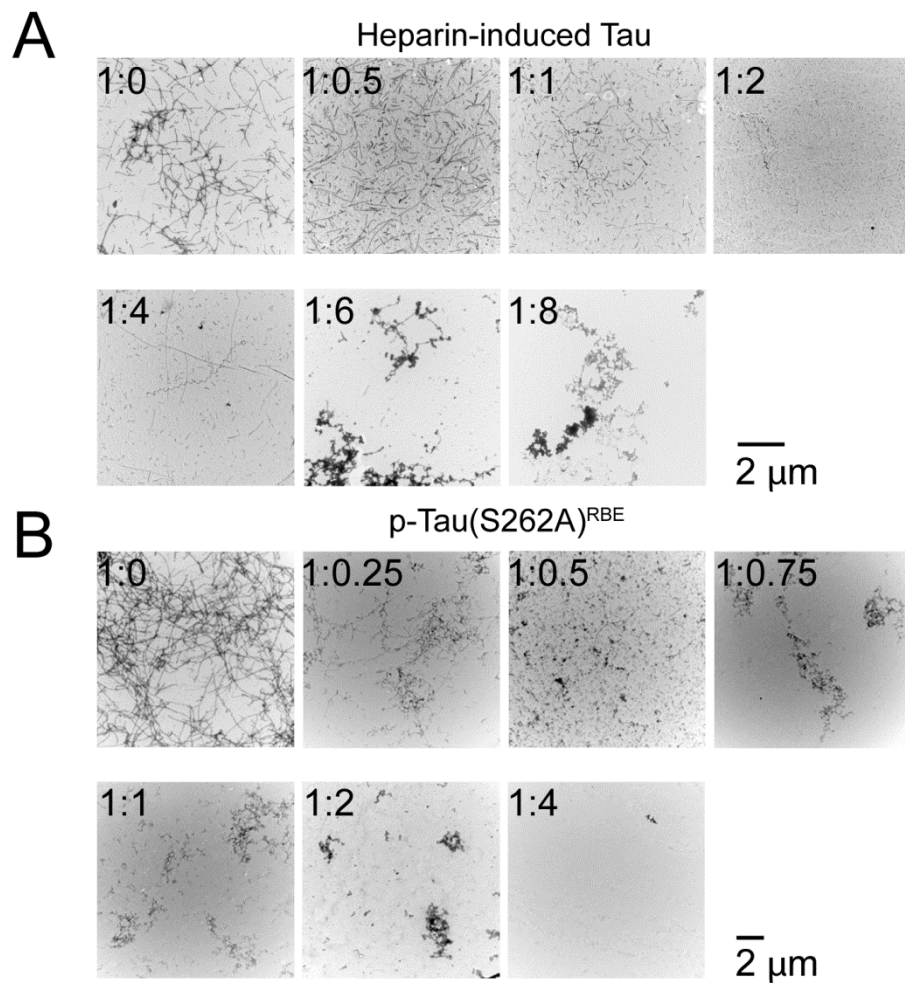
✉Corresponding authors: Caroline Smet-Nocca, [caroline.smet-nocca@univ-lille.fr](mailto:caroline.smet-nocca@univ-lille.fr) and Gal Bitan, [gbitan@mednet.ucla.edu](mailto:gbitan@mednet.ucla.edu)



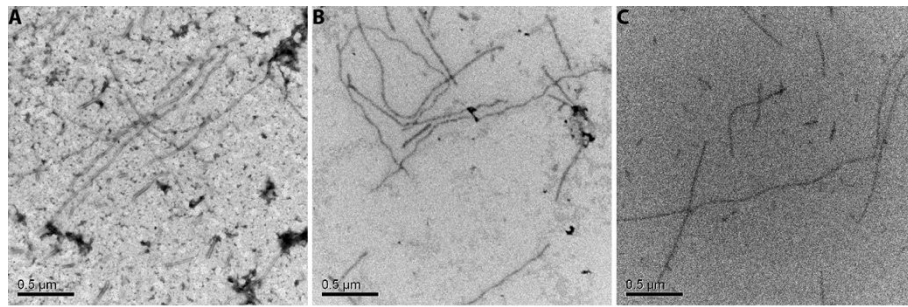
**Supplementary Figure S1.** Morphological examination by TEM at two different magnifications of p-tau(S262A)<sup>RBE</sup> fibrils obtained by incubation at 37°C of 30 μM of protein for 100 h.



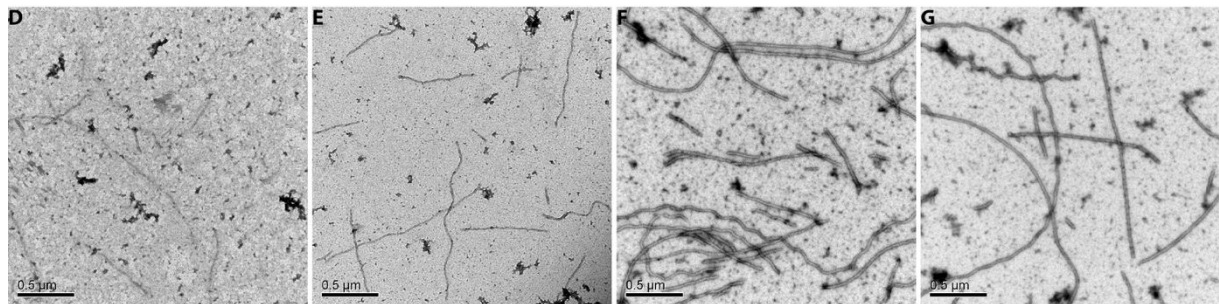
**Supplementary Figure S2.** Comparison of fitting the plateau vs. the rate constant,  $k$ , from aggregation kinetics curves for calculation of half-maximal inhibition by CLR01 of A) aggregation of unphosphorylated tau at  $5\mu\text{M}$  in the presence of  $1.25\mu\text{M}$  heparin, or B) aggregation of p-tau(S262A)<sup>RBE</sup> at  $30\mu\text{M}$ .



**Supplementary Figure S3.** Representative TEM images taken at the end of the aggregation reactions shown in Figure 5. A) Images of 5  $\mu\text{M}$  heparin-induced tau in the absence or presence of the indicated tau:CLR01 concentration ratios. B) Images of 30  $\mu\text{M}$  p-tau(S262A)<sup>RBE</sup> in the absence or presence of the indicated p-tau(S262A)<sup>RBE</sup>:CLR01 concentration ratios.

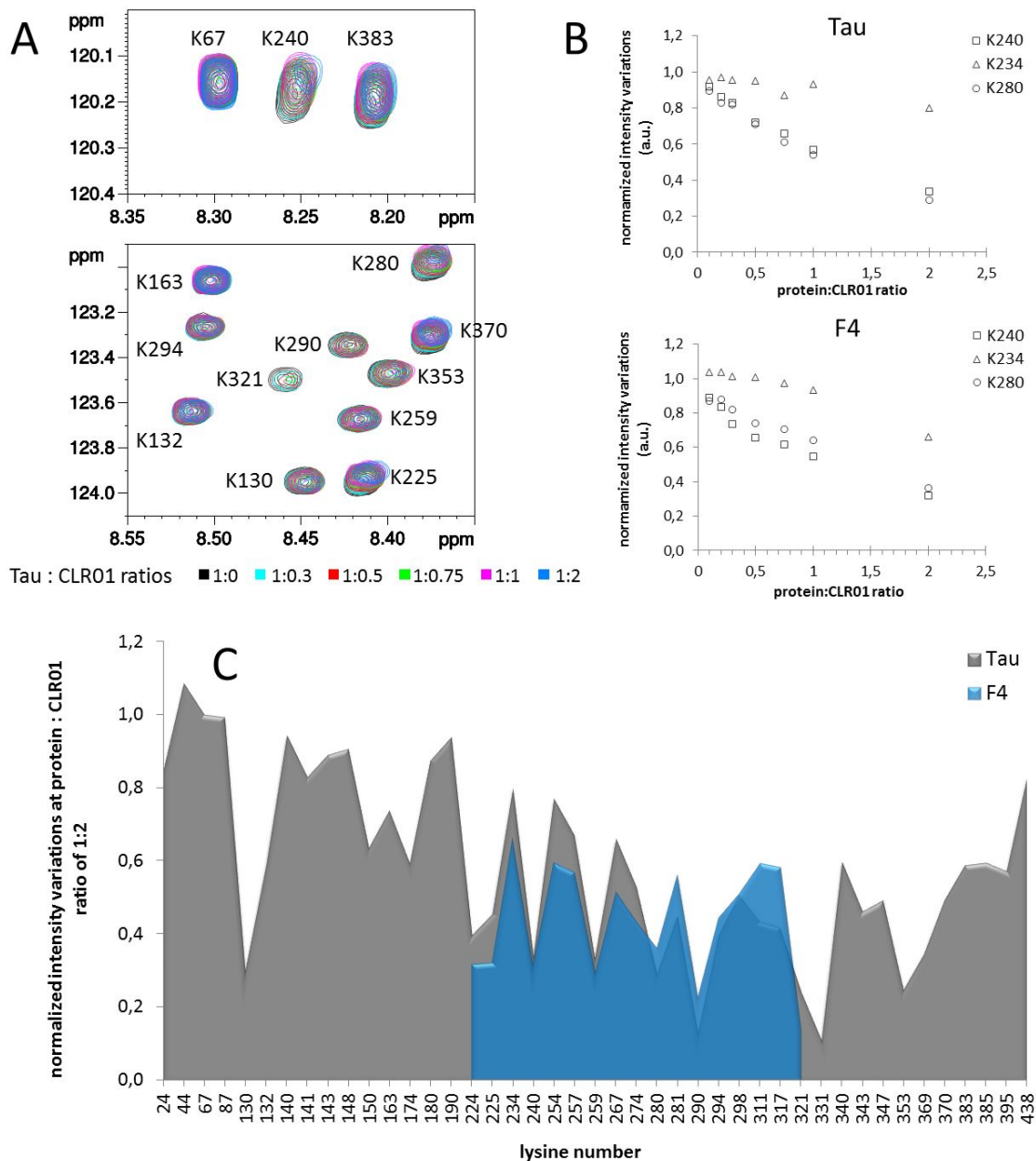


Sonication	-	+	+
24 h @ 37 °C	-	-	+
CLR01	-	-	-



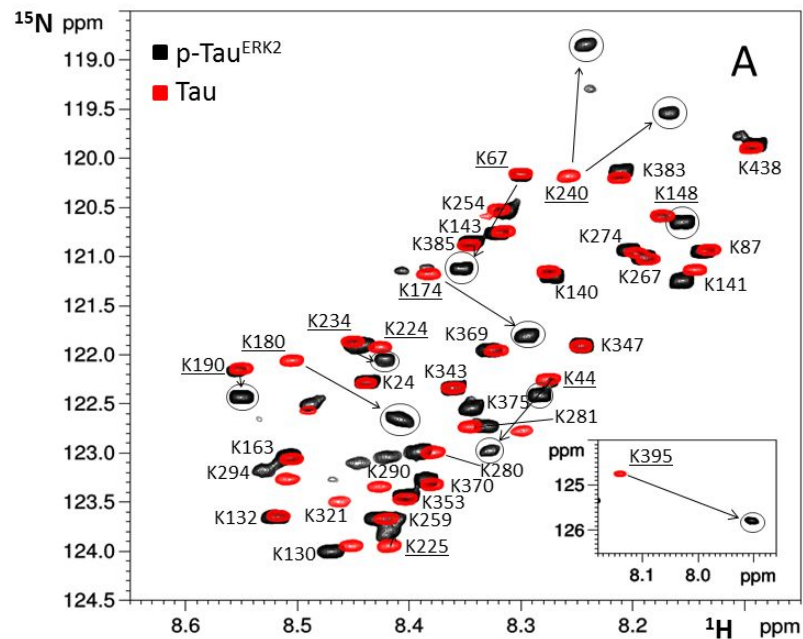
Sonication	+	+	+	+
24 h @ 37 °C	+	+	+	+
CLR01	1.5 μM	5 μM	15 μM	50 μM

**Supplementary Figure S4.** Transmission electron microscopy of p-tau(S262A)<sup>RBE</sup> fibrils in the absence or presence of different concentrations of CLR01. (A-C) p-Tau(S262A)<sup>RBE</sup> fibrils in the absence of CLR01 before sonication (A), after sonication (B), and after 24-h incubation at 37 °C followed by 10-min sonication (C). (D-G) p-Tau(S262A)<sup>RBE</sup> incubated for 24 h in the presence of 1.5 μM (D), 5 μM (E), 15 μM (F), or 50 μM (G) of CLR01 followed by 10-min sonication in each case.

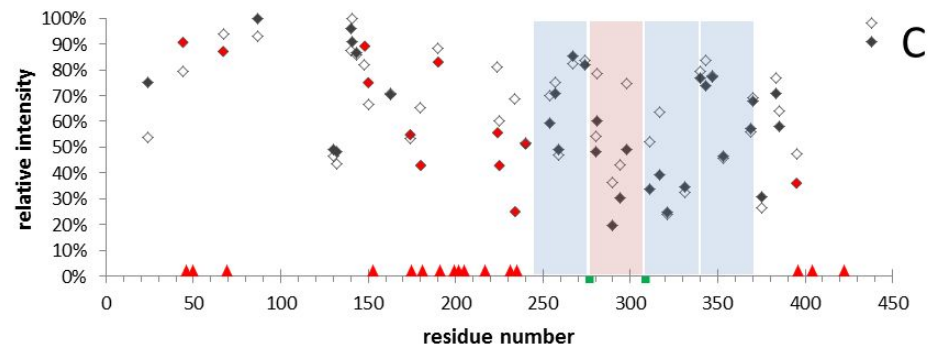


**Supplementary Figure S5. Titration of full-length tau and the F4 fragment with CLR01.** (A) Superimposition of  $^1\text{H}$ - $^{15}\text{N}$  HSQC spectra of  $^{15}\text{N}$ -Lys-tau for different tau:CLR01 concentration ratios. (B) Plots of the normalized resonance intensity variations for three interacting Lys residue K234, K240, K280 in full-length tau and F4. (C) Comparison of signal intensity variations at a two-fold excess of CLR01 for tau (grey) and F4 (blue) for each lysine residue in the tau sequence (longest isoform, 2N4R tau, numbering).



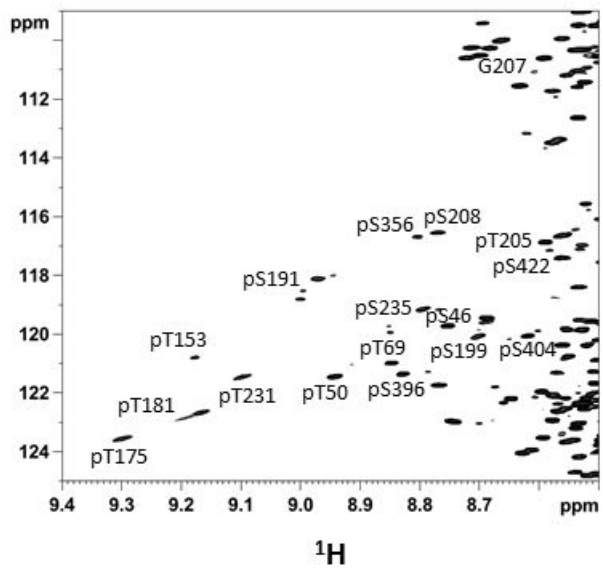
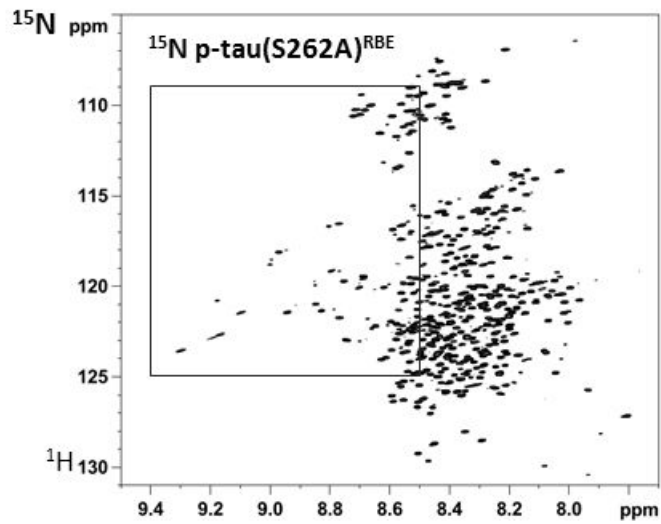


MAEPRQEFEV	MEDHAGTYGL	GDRKDQGGYT	MHQDQEGDTD	AGLKE <u>S</u> PLQT	PTEDGSEEPG	60
SETSDAK <u>S</u> T	TAEDVTAPLV	DEGAPGKQAA	AQPHEIPEG	TTAEEAGIGD	TPSLEDEAAG	120
HVTQARMVSK	SKDGTGSDDK	KAKGADGKT	<u>IAT</u> PRGAAPP	GQKGQANATR	IPAK <u>T</u> PPAPK	180
<u>T</u> PPSSGEPK	<u>S</u> GDRSGYSSP	<u>G</u> SPGT <u>P</u> GSRS	RTPSLP <u>T</u> PPT	REP <u>K</u> KVAVVR	<u>T</u> PK <u>S</u> PSSAK	240
SRLQTAPVPM	PDLKNVSKI	<u>G</u> STENLKHQP	<u>G</u> GK <u>VQ</u> IINK	<u>K</u> LDLSNVQSK	<u>C</u> GSKDNIKHV	300
<u>P</u> GGGS <u>VQ</u> IVY	<u>K</u> PVDLSKVTS	<u>K</u> CGSLGNIHH	<u>K</u> PGGGQVEVK	<u>S</u> EKLD <u>F</u> KDRV	<u>Q</u> SKIGSLDNI	360
<u>T</u> HV <u>P</u> GGGNKK	IETHKLTRE	NAKAKTDHGA	EIVY <u>K</u> SPVVS	GDT <u>S</u> PRHLSN	VSSTGSIDMV	420
<u>D</u> SPQLATLAD	EVSASLAKQG	L				441

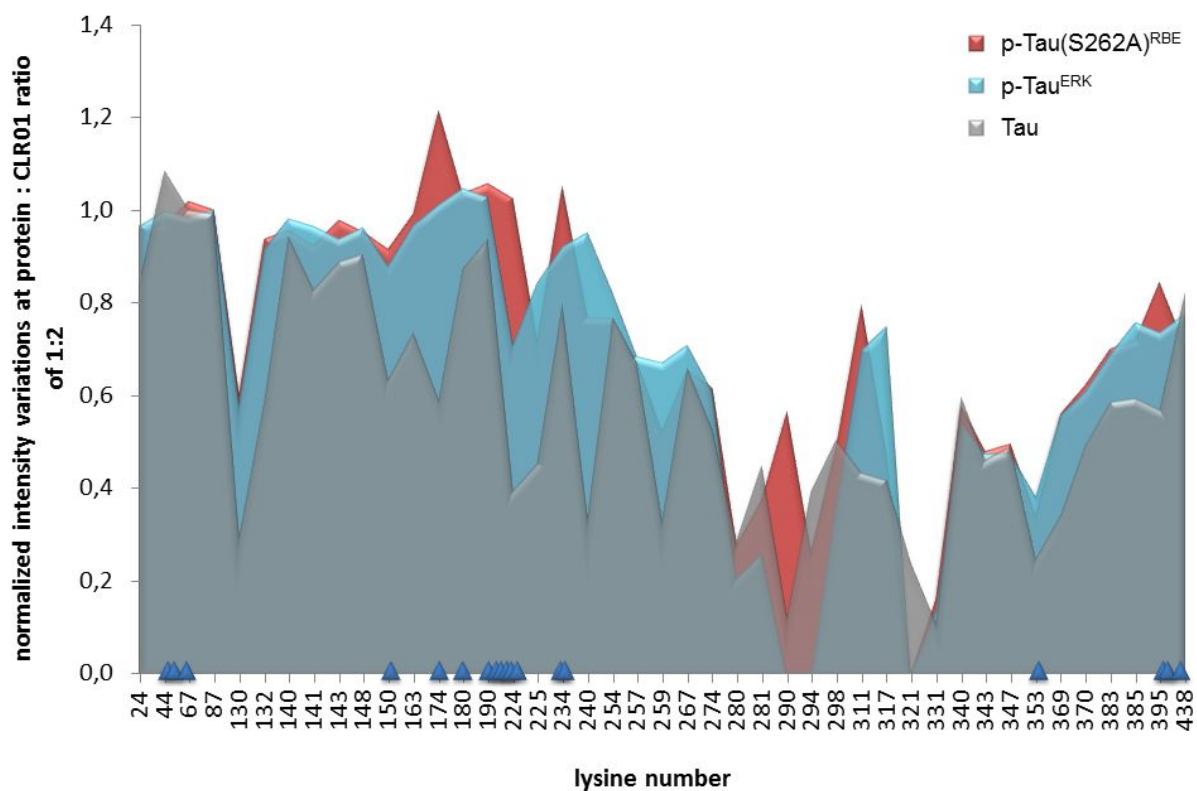


**Supplementary Figure S7. Phosphorylation of  $^{15}\text{N}$ -lysine, $^{13}\text{C}$ -tau by ERK2.** (A) Superimposition of  $^1\text{H}$ - $^{15}\text{N}$  HSQC spectra of p-tau<sup>ERK</sup> (black) and unphosphorylated ( $^{15}\text{N}$ -lysine, $^{13}\text{C}$ -tau) showing the effect of phosphorylation of lysine resonances that are in proximity of phosphorylation sites. (B) Sequence of tau in which ERK2 phosphorylation sites are annotated in red, additional RBE phosphorylation sites in blue and PHF6\* and PHF6 hexapeptides in green. R1, R3, R4 repeats are underlined in light blue and R2 in light red. Lys residues located in the neighborhood of phosphorylation sites are underlined. (C) Resonance intensity patterns of unphosphorylated tau (open diamonds) and p-tau<sup>ERK</sup> (filled diamonds). Lys residues close to phospho-sites are depicted by red filled diamonds. In the p-tau<sup>ERK</sup> sample, the sum of intensities of unphosphorylated and phosphorylated forms is plotted for Lys residues close to phospho-sites. Phosphorylation sites are indicated by red triangles. The hexapeptides PHF6\* and PHF6 in the R2 and R3 repeats are indicated by green lines. Regions corresponding to R1-R4 repeats are colored as indicated in (B).

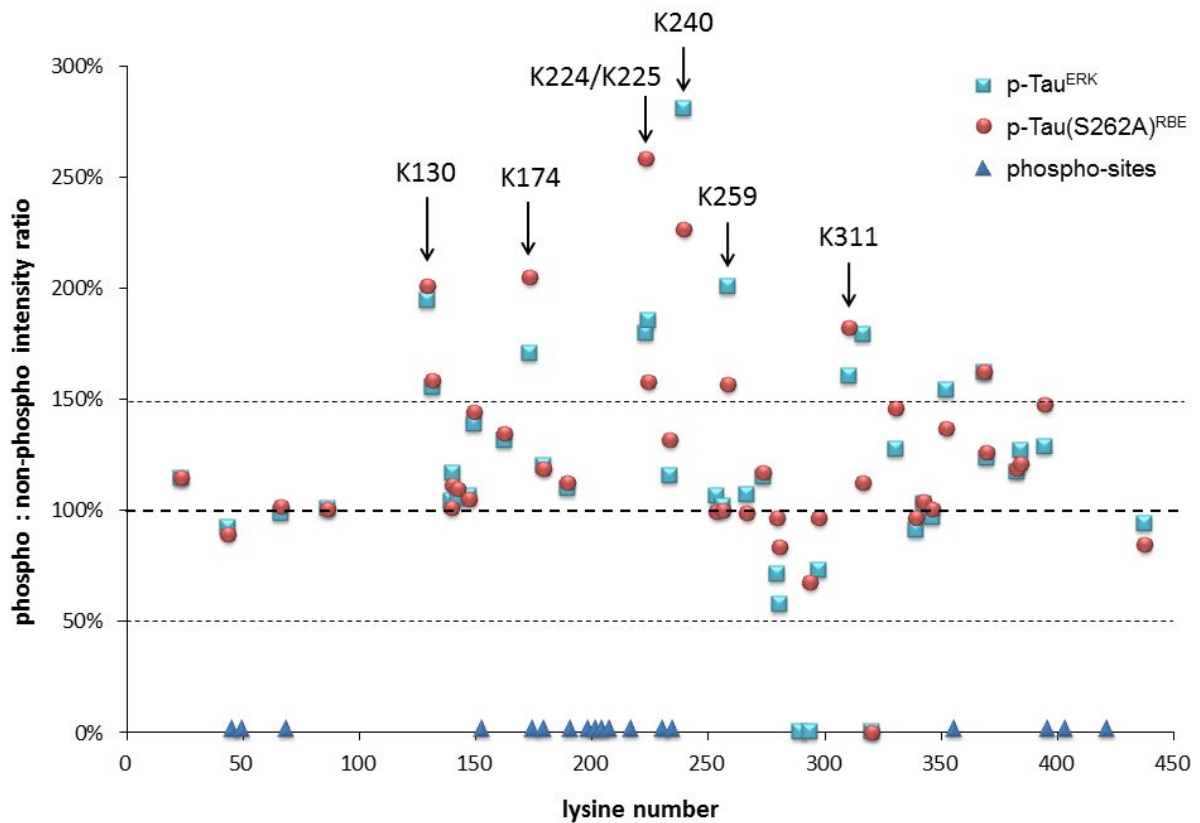




**Supplementary Figure S8.**  $^1\text{H}$ - $^{15}\text{N}$  HSQC spectra of p-tau(S262A)<sup>RBE</sup> phosphorylated by a rat brain extract. Lower panels correspond to the box regions in upper panels in which resonances of phosphorylation sites are annotated.



**Supplementary Figure S9.** Comparison of signal intensity variations in phosphorylated tau, p-tau<sup>ERK</sup> (cyan) and p-tau(S262A)<sup>RBE</sup> (red), and non-phosphorylated tau (grey) upon addition of a two-fold excess of CLR01. Intensity variations are plotted against lysine residues number along the tau sequence. Phosphorylation sites of p-tau(S262A)<sup>RBE</sup> are indicated by blue triangles.



**Supplementary Figure S10.** Ratio of signal intensity of phosphorylated tau, either p-tau<sup>ERK</sup> (cyan) or p-tau(S262A)<sup>RBE</sup> (red), on non-phosphorylated tau upon addition of a two-fold excess of CLR01. Intensity ratios are plotted against lysine residues number along the tau sequence. Phosphorylation sites of p-tau(S262A)<sup>RBE</sup> are indicated by blue triangles. Ratios higher than 100% indicate stronger interactions with non-phosphorylated tau while ratios lower than 100% indicate stronger interactions with phosphorylated tau. Lysine residues affected in their interaction with CLR01 by phosphorylation are annotated.